AJNR

Multiplanar MR and anatomic study of the mandibular canal.

K Ikeda, K C Ho, B H Nowicki and V M Haughton

AJNR Am J Neuroradiol 1996, 17 (3) 579-584
http://www.ajnr.org/content/17/3/579

This information is current as of August 13, 2025.

Multiplanar MR and Anatomic Study of the Mandibular Canal

Koshi Ikeda, Khang-Cheng Ho, Bruce H. Nowicki, and Victor M. Haughton

PURPOSE: To evaluate the MR appearance of the mandibular canal and its contents. **METHODS:** Cadaveric mandibles were imaged at 1.5 T and 3 T, then sectioned with a cryomicrotome. The size, shape, signal intensity, and pattern of structures in the mandibular canal were identified on MR images by comparing them with corresponding anatomic sections. **RESULTS:** The inferior alveolar nerve and connective tissue were identified on the 1.5-T and 3-T images in the mandibular canal. Within the nerve the axon bundles were distinguished from the nerve sheath on the 3-T images. **CONCLUSION:** This study suggests that MR images can show excellent anatomic detail in the mandibular canal.

Index terms: Temporomandibular joint, anatomy; Temporomandibular joint, magnetic resonance

AJNR Am J Neuroradiol 17:579–584, March 1996

Lesions of the inferior alveolar nerve (IAN) are common. Trauma to the IAN complicates some dental extractions (1, 2). Neoplastic infiltration of the IAN is the most common cause of dysesthesia or anesthesia in the face (3). Evaluation of traumatic or neoplastic lesions of the IAN is difficult because no effective imaging strategy has been developed. Radiographs do not consistently show the mandibular canal in which the nerve is located (4, 5). Computed tomography (CT) shows the canal but not the nerve or its branches (6, 7). Furthermore, the anatomy of the IAN is highly variable (8). We conducted a magnetic resonance (MR) and anatomic correlative study of the mandibular canal using a 1.5-T imager and, to achieve more detail and higher resolution, an experimental 3-T imager.

Materials and Methods

Six cadavers acquired from our institution's body donation program were frozen within 48 hours of death at −20°C. The mandible was removed en bloc from the frozen cadaver with a bandsaw and divided into left and right sections.

The hemimandibles were thawed at room temperature before imaging. Six were imaged in a 1.5-T imager with an experimental solenoid coil 10 cm in diameter. The specimens were placed in the 1.5-T unit such that the long axes were aligned with the y-axis and z-axis of the magnet. Spin-echo images were obtained in sagittal, axial, and coronal planes with parameters of 500/40/4 and 2000/70/2 (repetition time/echo time/excitations), a 512 × 256 matrix, a 1.0-mm section thickness, and a 16-cm field of view. The other six hemimandibles were imaged in a 3-T imager with an experimental solenoid coil 3.3 cm in diameter. The small cylindrical specimens imaged at 3 T were placed in the circular coil with the mandibular canal parallel to the axis of the coil and the coil aligned with the x-axis of the scanner. Spin-echo images were obtained in the coronal plane with parameters of 1500/60/4, a 256 × 256 matrix, a 1.0-mm section thickness, and a 3-cm field of view.

After imaging, each hemimandible was placed in styrofoam box under fluoroscopic monitoring to align the midportion of the mandibular canal parallel to the sides of the box. The box was then filled with aqueous carboxymethylcellulose solution and frozen. The frozen block containing the specimen was then placed on the stage of the cryomicrotome (Jung Cryo Macrocut, Leica Instruments Gmbh, Deerfield, Ill) and sectioned in sagittal, axial, or coronal planes. Sections 20 μm thick were removed from the surface of the specimen, and the surface of the specimen (on which a centimeter ruler was placed) was photographed (Olympus OM-2N and Kodachrome 100 ASA film) as each 0.5 mm of tissue was removed. The appearance of the nerves, arteries, and connective tissue in the mandibular canal in the Kodachrome slides were ana-

Received May 25, 1995; accepted after revision September 15.

From the Departments of Radiology (K.I., B.H.N., V.M.H.) and Pathology (K-C.H.), The Medical College of Wisconsin, Milwaukee.

Address reprint requests to Victor M. Haughton, MD, Department of Radiology, Medical College of Wisconsin, 8700 W Wisconsin Ave, Milwaukee, WI 53226.

AJNR 17:579–584, Mar 1996 0195-6108/96/1703–0579
© American Society of Neuroradiology

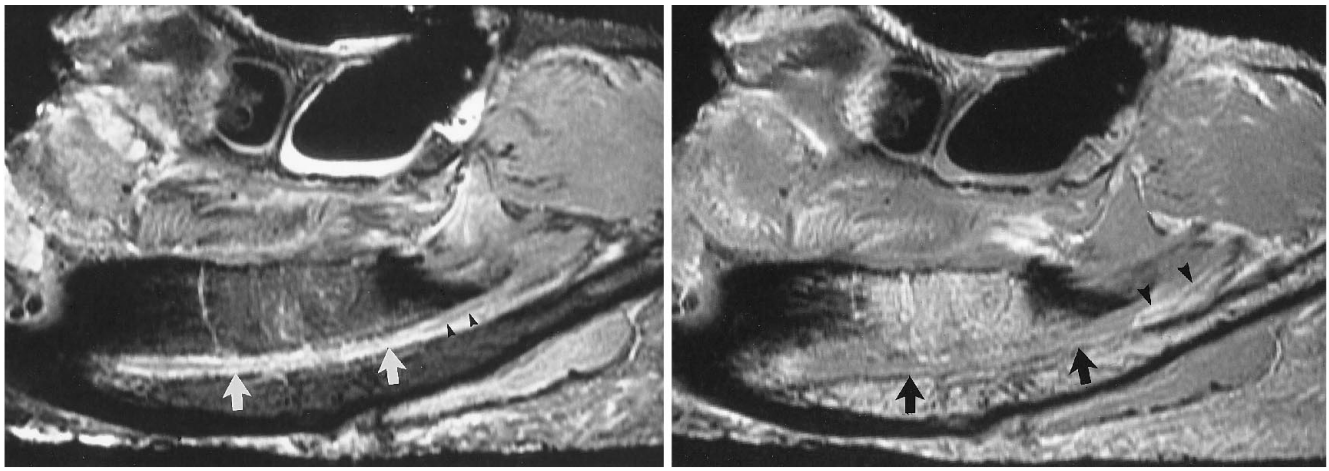

Fig 1. Sagittal T2-weighted MR image (*A*) of a cadaveric mandible shows the mandibular canal (*arrows*), the inferior alveolar nerve (*arrowheads*), and surrounding connective tissue, which has a higher signal intensity. In the corresponding T1-weighted MR image (*B*), the canal (*arrow*) and nerve (*arrowheads*) are shown, and the connective tissue has a higher signal intensity.

lyzed. The dimensions of the nerve were measured on the slides by means of a calipers and the centimeter index was included in each photograph. Four of the 12 specimens were sectioned sagittally, 2 axially, and 6 coronally.

Four of the blocs of tissue remaining after cryomicrotome sectioning were processed for histologic staining. The four blocs were fixed in 10% buffered formalin for 1 day and then decalcified in Dowex (an ion-exchange resin) solution for 6 weeks. Specimens were embedded in paraffin, sectioned on a microtome, and stained with hematoxylin-eosin stains and examined under light microscopy.

Results

On the MR images, the IAN and its branches were identified (Figs 1 and 2). The IAN within the mandibular canal typically had three branches. The first, or retromolar, branch separated from the IAN at the mandibular foramen, had a 2- to 5-mm course parallel to the IAN, and then turned upward, posterior to the third molar. The second, or molar, branch arose from the IAN or from the retromolar branch, and had a course parallel to the IAN before turning in a cephalad direction. The third, or incisor, branch arose adjacent to the mental foramen and then coursed anteriorly. In cross section, the mandibular canal near the mandibular foramen (Fig 3) in which the IAN and a portion of the retromolar branch were located was roughly oval in shape. The canal was round in cross section

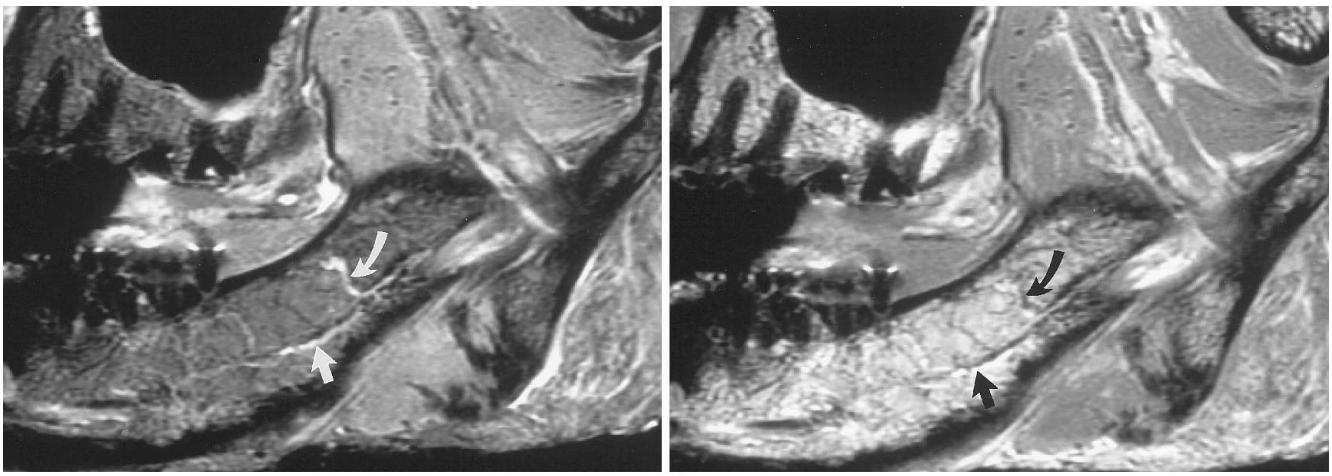

Fig 2. Sagittal T2-weighted (*A*) and T1-weighted (*B*) MR images, medial to the mandibular canal, show the molar branch (*straight arrow*) arising from the retromolar branch (*curved arrow*) and running parallel to the mandibular canal.

Fig 3. Coronal MR image at 3 T near the mandibular foramen in another cadaver illustrates the inferior alveolar nerve (*straight arrow*) and retromolar branch (*curved arrow*) in the mandibular canal.

near the middle of the canal (Fig 4). The greater diameter of the canal averaged 4.1 mm (SD, 0.5 mm) near the mandibular foramen. The average diameter of the canal was 3.4 mm (SD, 0.5 mm) in the middle of the canal. The mandibular canal contained the IAN, the inferior alveolar artery, loose connective tissue, and sometimes a portion of the retromolar or molar branch of the IAN. The IAN was oval or round and, on average, 2.2 mm (SD, 0.4 mm) in diameter. The inferior alveolar artery was identified parallel to the nerve in all cases. It was in the inferior portion of the mandibular canal near the mandibular foramen. Half the time it was located in the lateral inferior portion and half the time in the medial inferior portion. In the middle of the canal, it was located in the medial superior portion of the canal (Fig 4). The artery averaged 0.7 mm (SD, 0.2 mm) in diameter. The distance between the nerve and the nearest teeth ranged from 6 mm to 7 mm at the second molar.

The IAN on histologic section was inhomogeneous. The peripheral sheath (epineurium) of the nerve had a homogeneous fibrous structure. In the epineurium, the two to eight axon bundles

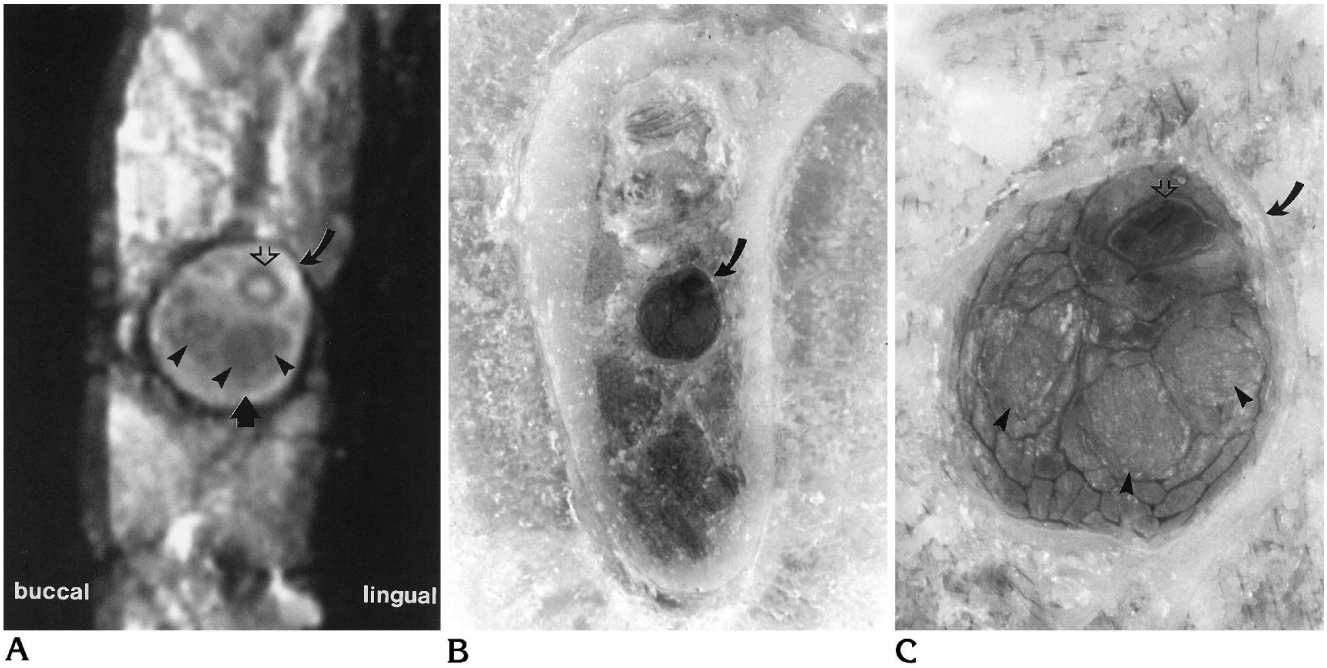

Fig 4. Comparison of a coronal MR image (1500/60/4) obtained at 3 T (*A*) with the corresponding cryomicrotome section (*B*) and magnification of the section at midcanal level (*C*). In the MR image, the osseous margins of the mandibular canal (*curved arrow*), the artery (*open arrow*), and the nerve (*straight arrow*) are seen. Within the nerve the axon bundles (*arrowheads*) and the sheath are identified. In the cryomicrotome sections, the osseous margin of the canal (*curved arrow*), the artery (*open arrow*), the nerve, and the axon bundles (*arrowheads*) are shown.

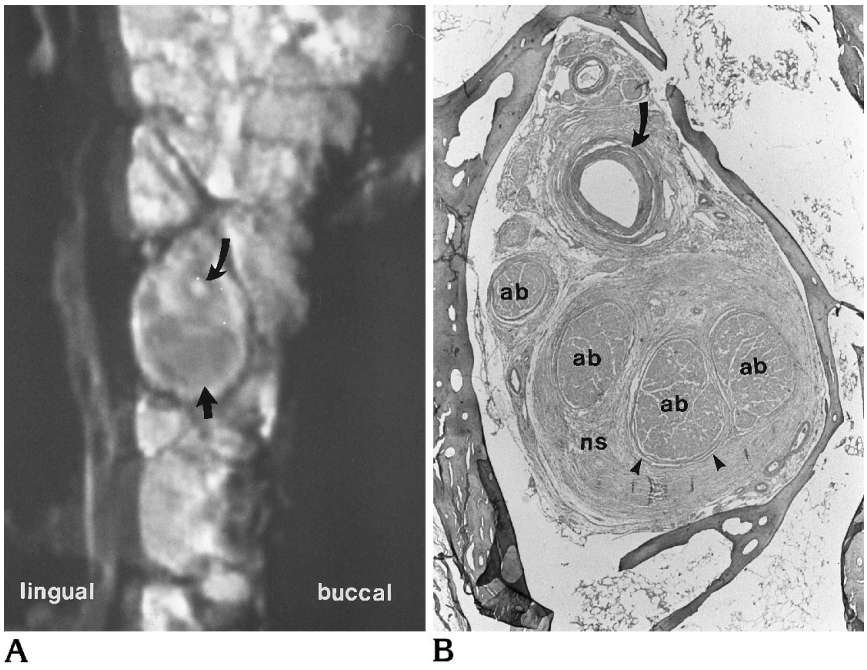

Fig 5. Comparison of the coronal 3-T MR image with corresponding histologic section. In the MR image (*A*), the artery (*curved arrow*) and nerve (*straight arrow*) are labeled. In the histologic section (*B*), the axon bundles (*ab*), nerve sheath (*ns*), perineurium (*arrowheads*), and artery (*curved arrow*) are labeled.

were oval, slightly irregular, and slightly inhomogeneous structures. Each of the axon bundles was enclosed in perineurium (Figs 5 and 6).

On T1-weighted and T2-weighted MR images at 1.5 T, the IAN in the mandibular canal had a low signal intensity, approximately isointense with the muscle. The connective tissue around the IAN had higher signal intensity on T1-weighted and T2-weighted images. The course of the IAN from the mandibular foramen to the mental foramen was evident on the sagittal images (Figs 1 and 2). It was identified more clearly on T2-weighted images than on T1-weighted images. The artery was not seen on the sagittal image. In the nerve, the axon bundles were not distinguished from the sheath at 1.5 T.

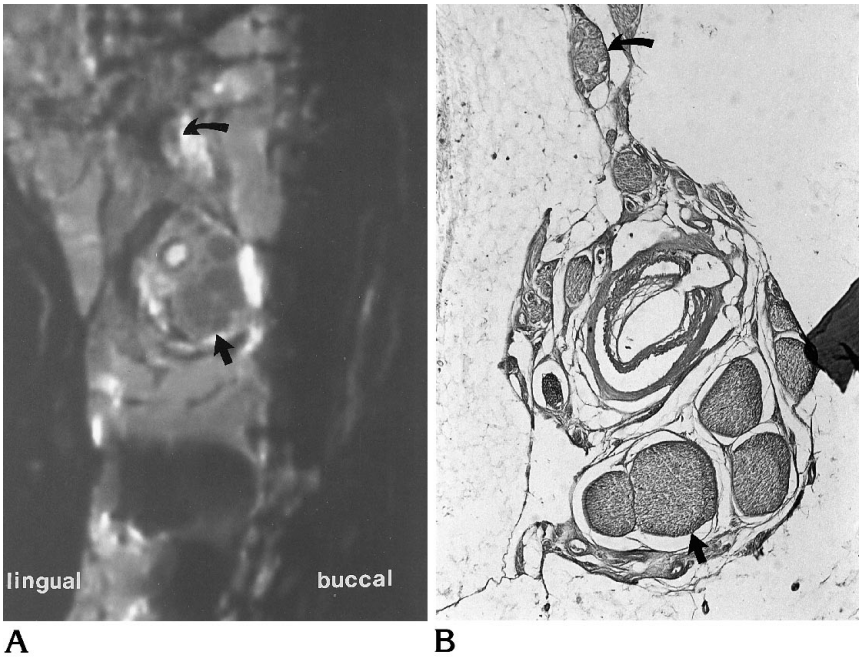

Fig 6. Comparison of the histologic section and coronal MR image obtained at 3 T in another cadaver shows the inferior alveolar nerve and the retromolar branch. In the MR image (*A*), the inferior alveolar nerve (*straight arrow*) and the retromolar branch (*curved arrow*) are labeled. Note that connective tissue of high signal intensity lies adjacent to the nerves. In the histologic section (*B*), the inferior alveolar nerve (*straight arrow*) and the retromolar branch (*curved arrow*) are shown.

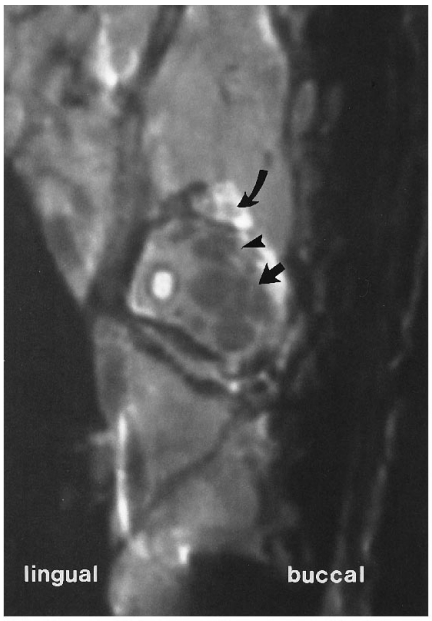

7

8

Fig 7. Coronal MR image obtained at 3 T near the mandibular foramen illustrates the inferior alveolar nerve (*straight arrow*) and the molar branch *(arrowhead*) in the mandibular canal and the retromolar branch outside the canal (*curved arrow*), distal to its branching from the inferior alveolar nerve. The high signal intensity in the canal is related to the lumen of the artery.

Fig 8. Coronal MR image obtained at 3 T posterior to the third molar illustrates the retromolar branch (*arrows*) exiting from the mandibular canal surrounded by connective tissue with a high signal intensity.

On the images acquired at 3 T (1500/60), the IAN was distinguished from the surrounding connective tissue of higher signal intensity. In the connective tissue, the inferior alveolar artery could be found as a low-signal-intensity structure with a higher signal intensity in the lumen. In the IAN, the axon bundles appeared as small irregularly shaped structures of lower signal intensity than that of the nerve sheath. The nerve sheath, which encircled the axon bundles, had a high signal intensity, comparable to bone marrow (Figs 5, 7, and 8).

Discussion

The cadaveric studies of the mandibular canal can be extrapolated to clinical imaging with some limitations. Postmortem, the contrast between tissues changes on MR images. Alanen et al (9) showed that a rat muscle stored in a refrigerator at 6°C had a significantly shorter T1 signal 1 day after death, which returned to baseline levels within 4 days after death. Since in our study the cadaver was stored several days at −20°C, the postmortem changes are probably not a significant factor. Freezing of cadaveric tissue does not change the anatomic relationships markedly. In freezing, the volume of tissue is changed by up to 7%; however, the volume change is most likely reversed by thawing for MR imaging (10). Since we used an experimental coil and scanner, we could demonstrate more detail in the mandibular canal than can be achieved clinically at the moment.

The transient neurologic disturbance of sensation in the lip and chin that follows tooth extraction in some cases presumably represents edema or damage to the IAN (2). An MR study of the mandible may reveal the anatomic relationships of the nerve and the teeth in the mandible and may help determine the risk of injury to the nerve from extraction. The location of the canal suggests that tooth extraction may damage either the artery or nerve. MR imaging of the IAN may help determine the cause of anesthesia after dental extraction.

In earlier studies of the nerve, variations of the IAN have been described. Previous authors have reported that the IAN divided into two branches, one supplying the molar, premolar, and canine teeth and the other the incisor teeth (8, 11, 12). Some authors described the IAN as dividing in the mandibular foramen, with the retromolar branch passing through a foramina in the retromolar fossa (13, 14). Schejtman et al (15) named this the mandibular retromolar canal. We found, as Hosaka (8) reported, that the IAN divided into three major branches in the mandibular canal, the ramus retromolaris, the rami molares, and the ramus incisivus. We also found that the artery in the mandibular canal occupied the medial superior portion of the canal near the mental foramen, in agreement with some authors (16–18). Like Mozsary and Syers

(19), we found that there are 2 to 8 fascicles per IAN, not 6 to 18, as others reported (20).

Some authors report that tumor invades along the IAN because the nerve is not tightly confined within the canal and foramen. Therefore, tumor spread into the canal may obliterate the high signal intensity of the connective tissue (21, 22). Our histologic findings that there is room between the IAN and the canal (Figs 3B and 4B) is supportive of this observation. The appearance of the canal in cases with tumor involvement should be studied. MR imaging may be useful in the diagnosis of tumor infiltrations of the IAN.

Another application of MR imaging of the IAN may be to facilitate a surgical anastomosis of the IAN. MR imaging may help in the selection of a donor nerve with similar fascicular size and patterns to the host nerve (20) and in the determination of the length of the nerve segment that is damaged.

Conclusion

The IAN can be shown effectively by MR imaging. Imaging the IAN and the artery with MR may help in determining the risk of injury to the nerve from tooth extraction, in diagnosing neoplastic infiltration in cases of metastatic carcinoma, and in facilitating microsurgery on the IAN.

References

1. Kipp DP, Goldstein BH, Weiss WW. Dysesthesia after mandibular third molar surgery: a retrospective study and analysis of 1377 surgical procedures. *J Am Dent Assoc* 1980;100:185–192
2. Osborn TP, Frederickson G, Small IA, Torgerson TS. A prospective study of complications related to mandibular third molar surgery. *J Oral Maxillofac Surg* 1985;43:767–769
3. Horowitz SH. Isolated facial numbness: clinical significance and relation to trigeminal neuropathy. *Ann Int Med* 1974;80:49–53
4. Stockdale CR. The relationship of the roots of mandibular third molars to the inferior dental canal. *Oral Surg Oral Med Oral Pathol* 1959;12:1061–1072
5. Littner MM, Kaffe I, Tamse A, Dicapua P. Relationship between the apices of the lower molars and mandibular canal: a radiographic study. Oral Surg *Oral Med Oral Pathol* 1986;62:595–602
6. Abrahams JJ. Anatomy of the jaw revisited with a dental CT software program. *AJNR Am J Neuroradiol* 1993;14:979–990
7. Feifel H, Reidiger D, Gustorf-Aeckerle R. High resolution computed tomography of the inferior alveolar and lingual nerves. *Neuroradiology* 1994;36:236–238
8. Hosaka N. The anatomical study of the submaxillary nerve in Japanese cadavers: the intra-mandibular course of the inferior alveolar nerve (in Japanese). *Shikagakuho J Tokyo Dent Col Soc* 1960;60:255–283
9. Alanen AM, Parkkola RK, Lillsunde IGV, et al. The effects of the method of death and lapsed time on proton relaxation time T1 in autopsied muscle samples. *Invest Radiol* 1993;28:529–532
10. Pech P, Bergström K, Rauschning W, Haughton VM. Attenuation values, volume changes and artifacts in tissue due to freezing. *Acta Radiol* 1987;28:779–782
11. Olivier E. The inferior dental canal and its nerve in the adult. *Br Dent J* 1928;49:356–358
12. Starkie C, Stewart D. The intra-mandibular course of the inferior dental nerve. *J Anat* 1931;65:319–323
13. Dieck W, Fujita T. Die Nerven der Kiefer und des Zahnfleisches beim Menschen mit vergleichsuntersuchung der verhältnisse beim Hunde (in German). *Gegenbaurs Morph Jahrb* 1935;76:570–588
14. Carter RB, Keen EN. The intramandibular course of the inferior alveolar nerve. *J Anat* 1971;108:433–440
15. Schejtman R, Devoto FCH, Arias NH. The origin and distribution of the elements of the human mandibular retromolar canal. *Arch Oral Biol* 1967;12:1261–1267
16. Oikarinen VJ. The inferior alveolar artery. *Suom Hammaslääk Toim* 1965;61(Suppl 1):1–131
17. Poirot G, Delattre JF, Palot C, Flament JB. The inferior alveolar artery in its bony course. *Surg Radiol Anat* 1986;8:237–244
18. Zoud K, Doran GA. Microsurgical anatomy of the inferior alveolar neurovascular plexus. *Surg Radiol Anat* 1993;15:175–179
19. Mozsary PG, Syers CS. Microsurgical correction of the injured inferior alveolar nerve. *J Oral Maxillofac Surg* 1985;43:353–358
20. Svane TJ, Wolford LM, Milam SB, Bass RK. Fascicular characteristics of the human inferior alveolar nerve. *J Oral Maxillofac Surg* 1986;44:431–434
21. Harris CP, Baringer JR. The numb chin in metastatic cancer. *West J Med* 1991;155:528–531
22. Matzko J, Becker DG, Phillips CD. Obliteration of fat planes by perineural spread of squamous cell carcinoma along the inferior alveolar nerve. *AJNR Am J Neuroradiol* 1994;15:1843–1845